Determination of the ionization and dissociation energies of the hydrogen molecule

Liu, J.J.; Salumbides, E.J.; Hollenstein, U.; Koelemeij, J.C.J.; Eikema, K.S.E.; Ubachs, W.M.G.; Merkt, F.

published in
Journal of Chemical Physics
2009

DOI (link to publisher)
10.1063/1.3120443

document version
Publisher's PDF, also known as Version of record

Determination of the ionization and dissociation energies of the hydrogen molecule

Jinjun Liu,[1] Edcel J. Salumbides,[2] Urs Hollenstein,[1] Jeroen C. J. Koelemeij,[2] Kjeld S. E. Eikema,[2] Wim Ubachs,[2] and Frédéric Merkt[1,a)]
[1]*Laboratorium für Physikalische Chemie, ETH-Zürich, 8093 Zürich, Switzerland*
[2]*Department of Physics and Astronomy, Laser Centre, Vrije Universiteit, De Boelelaan 1081, 1081 HV Amsterdam, The Netherlands*

(Received 19 December 2008; accepted 27 March 2009; published online 6 May 2009)

The transition wave number from the $EF\ ^1\Sigma_g^+(v=0,N=1)$ energy level of ortho-H_2 to the $54p1_1(0)$ Rydberg state below the $X^+\ ^2\Sigma_g^+(v^+=0,N^+=1)$ ground state of ortho-H_2^+ has been measured to be $25\ 209.997\ 56 \pm (0.000\ 22)_{\text{statistical}} \pm (0.000\ 07)_{\text{systematic}}$ cm^{-1}. Combining this result with previous experimental and theoretical results for other energy level intervals, the ionization and dissociation energies of the hydrogen molecule have been determined to be 124 417.491 13(37) and 36 118.069 62(37) cm^{-1}, respectively, which represents a precision improvement over previous experimental and theoretical results by more than one order of magnitude. The new value of the ionization energy can be regarded as the most precise and accurate experimental result of this quantity, whereas the dissociation energy is a hybrid experimental-theoretical determination.
 [DOI: 10.1063/1.3120443]

I. INTRODUCTION

The hydrogen molecule is an important system for testing molecular quantum mechanics. Both the ionization energy (E_i) and the dissociation energy (D_0) of H_2, related to each other by

$$D_0(H_2) = E_i(H_2) + D_0(H_2^+) - E_i(H), \tag{1}$$

are benchmark quantities for *ab initio* calculations and have played a fundamental role in the validation of molecular quantum mechanics and quantum chemistry and in the understanding of what chemical bonds really are.[1] The precision of both quantities has been improved by more than an order of magnitude over the past 3 decades (Refs. 2 and 3 and references therein), and the latest experimental values [$E_i(H_2)_{\text{exp}}$=124 417.476(12) cm^{-1} (Ref. 2) and $D_0(H_2)_{\text{exp}}$ =36 118.062(10) cm^{-1} (Ref. 3)] are compatible with the latest theoretical ones [$E_i(H_2)_{\text{th}}$=124 417.491 cm^{-1} and $D_0(H_2)_{\text{th}}$=36 118.069 cm^{-1} (Ref. 4)]. A new measurement of either $E_i(H_2)$ or $D_0(H_2)$ with improved precision would be desirable to test current and future theoretical calculations of either $E_i(H_2)$ or $D_0(H_2)$.

In this article, we report on a new experimental determination of the ionization energy of ortho-H_2 as a sum of three energy intervals: the first between the $X\ ^1\Sigma_g^+(v=0,N=1)$ and the $EF\ ^1\Sigma_g^+(v=0,N=1)$ levels of ortho-H_2 [99 109.731 39(18) cm^{-1} (Ref. 5)], the second between the $EF\ ^1\Sigma_g^+(v=0,N=1)$ and $54p$ Rydberg states belonging to series converging on the $X^+\ ^2\Sigma_g^+(v^+=0,N^+=1)$ level of ortho-H_2^+, and the third between the selected $54p1_1(0)$ Rydberg state and the center of gravity of the $X^+\ ^2\Sigma_g^+(v^+=0,N^+=1)$ ionic level [37.509 02(2) cm^{-1} (Ref. 6)]. We present here a measurement of the second energy interval, which when combined with the other two, enables us to derive a more precise value of the ionization energy of ortho-H_2. The ionization energy $E_i(H_2)$ and the dissociation energy $D_0(H_2)$ of para-H_2 can also be derived from this new measurement by including previous results on the ionization energy of the hydrogen atom,[7] the dissociation energy of H_2^+,[4] and the rotational energy level intervals for the lowest vibronic states of the neutral molecule and the cation.[8–11]

II. EXPERIMENT

The experiment was carried out using a two-step excitation scheme (bold arrows in Fig. 1). A pulsed supersonic beam of molecular hydrogen (2 bar stagnation pressure) was collimated by a 0.5-mm-diameter skimmer before it entered a differentially pumped ($\sim 10^{-7}$ mbar) interaction region, where it was crossed at right angles by two laser beams. In the first step, H_2 was excited from the $X\ ^1\Sigma_g^+(v=0,N=1)$ level to the $EF\ ^1\Sigma_g^+(v=0,N=1)$ level in a nonresonant two-photon process using a UV laser (wavelength of 202 nm, bandwidth of $\sim$0.4 cm^{-1}, pulse length of $\sim$10 ns, and pulse energy of $\sim$20 μJ). The UV radiation was generated by frequency upconversion of the output of a pulsed dye laser in two β-barium borate crystals. The broad bandwidth served the purpose of exciting all Doppler components of the transition and so avoiding the systematic shift of the wave numbers of the transitions from the $EF\ ^1\Sigma_g^+(v=0,N=1)$ state to the high Rydberg states that would result from selecting a subset of the hydrogen molecules with nonzero Doppler shifts. A possible residual effect caused by an asymmetric intensity profile across the Doppler lineshape would in any case cancel out when determining the transition frequencies as the average of two measurements carried out with counterpropagating beams (see below).

a)Electronic mail: feme@xuv.phys.chem.ethz.ch.

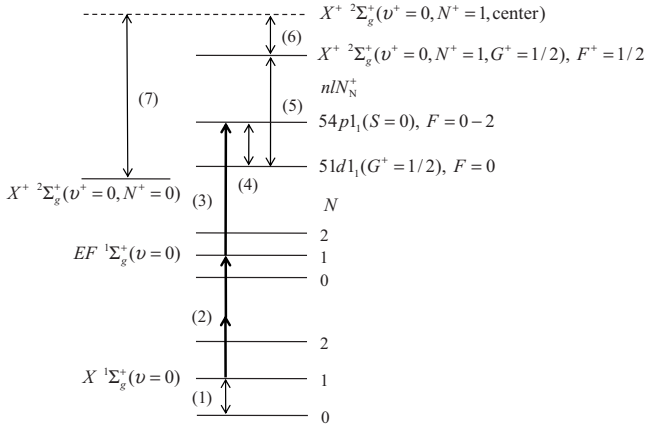

FIG. 1. Schematic energy level diagram of H_2 illustrating the procedure used to determine the ionization energy of H_2. The energy intervals are not to scale. The bold arrows show the multiphoton excitation scheme used in the present experiment.

In the second step, H_2 was excited from the $EF\ ^1\Sigma_g^+(v=0,N=1)$ level to the $54p$ Rydberg states located below the $X^+\ ^2\Sigma_g^+(v^+=0,N^+=1)$ ionic state using a second UV laser (wavelength of 397 nm, bandwidth of ~20 MHz, pulse length of ~50 ns, and pulse energy of ~40 μJ). The UV radiation for the second step was the second harmonic of the output of a pulsed titanium-doped sapphire (Ti:Sa) amplifier.[12,13] The single-mode output of a Ti:Sa cw ring laser was shaped into pulses by an acousto-optic modulator and used as the seed source of the Ti:Sa amplifier. The 397 nm laser was delayed by 50 ns with respect to the 202 nm laser. To measure the Doppler shift resulting from a possible nonorthogonality between the molecular hydrogen beam and the 397 nm laser beam, the 397 nm laser beam was split into two components by a 50% beam splitter. A dichroic mirror was used to overlap one of the two components with the 202 nm laser, while the other was introduced into the interaction region in a counterpropagating configuration. The difference between the transition wave numbers measured using each of these two components represents twice the Doppler shift, which can be eliminated by taking the average value of the two measurements. Both the 202 and 397 nm laser beams were slightly focused to a spot size of ~1 mm^2 in the interaction region. The molecules in Rydberg states created by the two-step excitation were ionized by applying a pulsed voltage delayed by 150 ns with respect to the 397 nm laser pulse across a set of seven resistively coupled metallic plates. H_2^+ was extracted by the same pulsed electric field and detected by a microchannel plate detector. The experimental region was surrounded by a double layer of mu-metal magnetic shielding to eliminate stray magnetic fields.[14]

III. RESULTS

A. The $54p1_1(0)[X\ ^2\Sigma_g^+(v^+=0,N^+=1)] \leftarrow EF\ ^1\Sigma_g^+(v=0,N=1)$ transition of H_2

Figure 2 shows two field ionization spectra of ortho-H_2 in the region of the transitions from the $EF\ ^1\Sigma_g^+(v=0,N=1)$ level to the $54p$ Rydberg states located below the $X^+\ ^2\Sigma_g^+(v^+=0,N^+=1)$ ionic state recorded with pulse energies of 700 μJ (panel a) and 40 μJ (panel b). The final states of these transitions are labeled using the notation $nlN_N^+(S)$, where the quantum numbers have their usual meaning.[6] The wave numbers are given relative to the $X\ ^1\Sigma_g^+(v=0,N=0)$ ground state and correspond to the sum of the wave number intervals between the $N=0$ and $N=1$ rotational levels of the $X\ ^1\Sigma_g^+(v=0)$ ground state, 118.486 84(10) cm^{-1} (Ref. 8), between the $X\ ^1\Sigma_g^+(v=0,N=1)$ and the $EF\ ^1\Sigma_g^+(v=0,N=1)$ levels, 99 109.731 39(18) cm^{-1} (Ref. 5), and between the $EF\ ^1\Sigma_g^+(v=0,N=1)$ level and the $54p$ Rydberg states. In the spectrum recorded at high laser power [Fig. 2(a)] more lines are observed than in that recorded at low power [Fig. 2(b)]. The additional lines in Fig. 2(a) correspond to weak

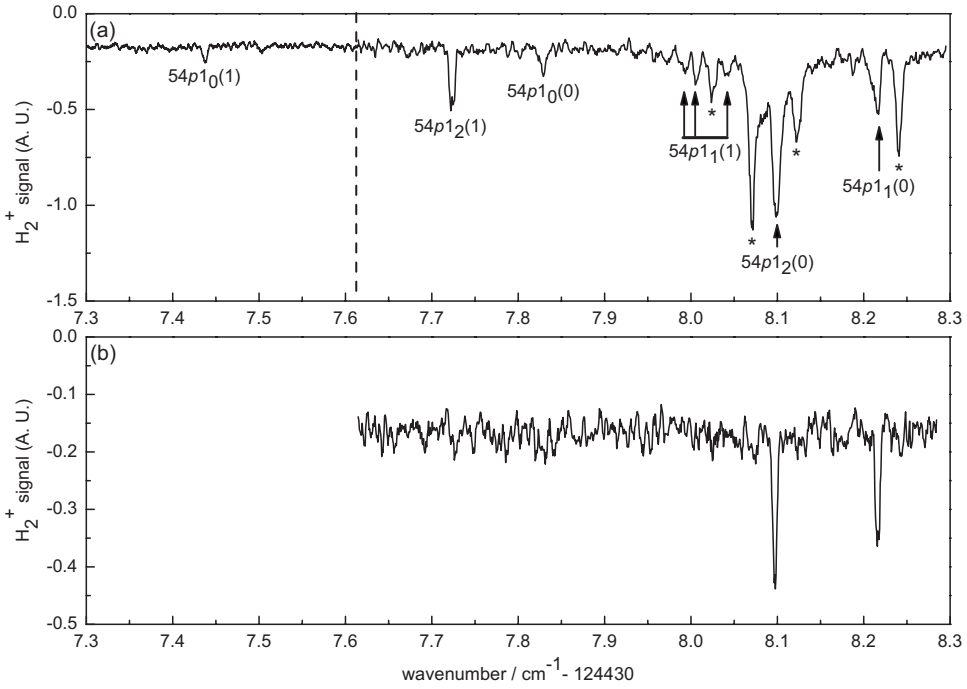

FIG. 2. Field ionization spectra of H_2 in the region of transitions to the $54p$ Rydberg states recorded using 397 nm laser pulse energies of (a) 700 μJ and (b) 40 μJ. The vertical dashed line indicates the junction point of two different scans. The scan on the low wave number side was taken with a smaller frequency step size and more averaging for each data point to increase the signal-to-noise ratio. The wave numbers are given relative to the position of the $X\ ^1\Sigma_g^+(v=0,N=0)$ ground state of para-H_2.

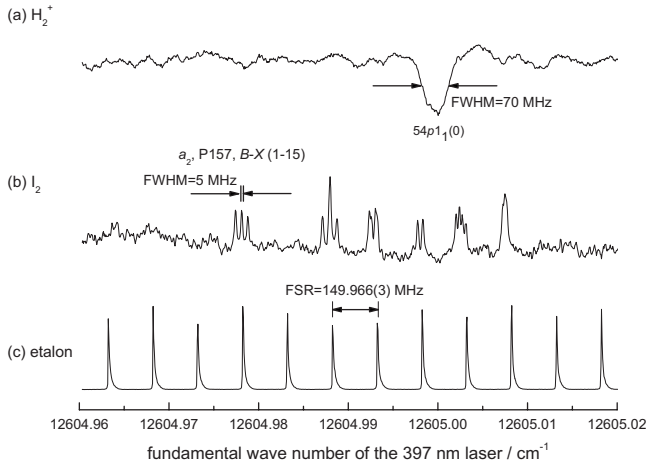

FIG. 3. Spectrum showing the transition from the $EF\ ^1\Sigma_g^+(v=0,N=1)$ level to the $54p1_1(0)$ level (a) with the I_2 calibration (b) and etalon (c) traces. The position of the a_2 hyperfine component of the P157, $B-X$ (1–15) rovibronic transition of I_2 was determined to be at 377 886 781.37(10) MHz using a frequency comb.

transitions, for instance, transitions to triplet Rydberg levels. Most of the observed lines could be assigned by comparing with the results of multichannel quantum defect theory calculations.[6] The assignment of the four lines marked by asterisks remains uncertain and requires further calculations. Only two lines are observed at low laser power. These two lines can be unambiguously assigned to the two allowed transitions to the $54p1_2(0)$ and $54p1_1(0)$ levels. For the present determination of the ionization energy of H_2, we chose to use the latter transition because the binding energy of the $54p1_1(0)$ level was determined with an absolute accuracy of ~600 kHz in Ref. 6.

For the calibration procedure, part of the output of the cw Ti:Sa laser was directed into an I_2 cell and through a high-finesse Fabry–Pérot (FP) etalon. The absolute frequency was calibrated by recording, simultaneously with each spectrum, the Doppler-free saturation absorption spectrum of I_2 using a 75-cm-long cell heated to 900 K.[5,15] The frequencies of the hyperfine components of the I_2 transitions were determined with an accuracy of better than 100 kHz by comparing with positions measured using a frequency comb[5] in a separate measurement. The H_2 spectra were linearized using the transmission signal through the FP etalon by cubic spline interpolation. The FP etalon was locked to a polarization-stabilized He–Ne laser, and its free spectral range (FSR) was determined with an accuracy of 3 kHz using two iodine lines.

To compensate for a possible chirp or shift in the near infrared (NIR) pulse arising in the multipass amplification in the Ti:Sa crystals, we have carried out a measurement of the frequency evolution during the pulse by monitoring the beating of the pulsed amplified beam with the cw NIR output of the ring laser as explained in Ref. 12 and determining the optical phase evolution following the procedure described in Ref. 16. The measurement yielded a frequency shift of −4.76(60) MHz with no significant chirp during the pulse. We attribute this shift to an optical effect caused by the depletion of the excited state population. Numerical modeling of the frequency characteristics of the pulse following the procedure discussed in Ref. 17 and using optical data on Ti:Sa crystals from Refs. 18 and 19 reproduced the observed shift (and the absence of a chirp) semiquantitatively. Indeed, our numerical simulation predicted a shift of about −3 MHz under our experimental conditions. The missing factor of about 1.6 could be explained by the uncertainty in the Nd:YAG pump fluence. The fact that we observed a frequency shift rather than a chirp under the present experimental conditions is attributed to the nearly constant rate of depopulation of the excited state when a sufficiently low pump power is used.

The centers of the lines in the H_2 spectra were determined by fitting a Gaussian lineshape function to each transition. An example illustrating the calibration of the transition to the $54p1_1(0)$ level is shown in Fig. 3. Sixteen pairs of measurements were carried out on 4 different days, each pair consisting of two scans, one recorded with the 397 nm laser beam propagating parallel and the other antiparallel to the 202 nm laser beam. The transition frequencies determined from these measurements are plotted with their uncertainties

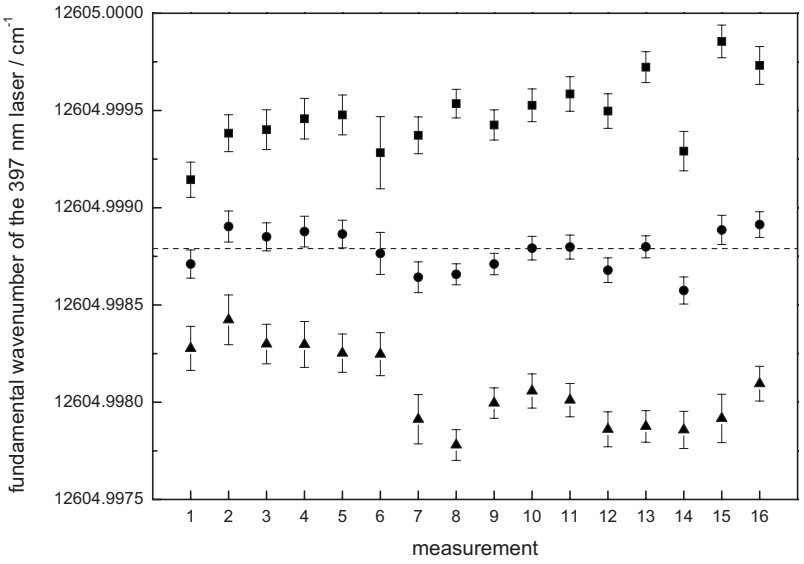

FIG. 4. Distribution of the calibrated fundamental wave numbers for the transition to the $54p1_1(0)$ level. Triangles and squares are measurements with two counterpropagating 397 nm laser beams, respectively. Closed circles are mean values of pairs of measurements. The dashed line marks the position of the overall mean value (12 604.998 80(10) cm^{-1}).

TABLE I. Error budget. Individual corrections and errors were determined for the frequency of the cw Ti:Sa laser and are thus multiplied by two.

Statistical uncertainties	Value (MHz)
Uncertainty in the determination of the line centers:	
I_2 spectra	$\pm 0.36 \times 2$
H_2 spectra	$\pm 3.0 \times 2$
Nonlinearity of the ring laser scans	$< \pm 1.1 \times 2$
Residual Doppler shift	$< \pm 0.32 \times 2$
Sum in quadrature	± 6.5
Systematic shifts and uncertainties	**Value (MHz)**
Error in linearization due to uncertainty of FSR	$\pm 0.012 \times 2$
Uncertainty in the positions of the I_2 reference lines[a]	$< \pm 0.1 \times 2$
Frequency shift in the Ti:Sa amplifier	$(-4.76 \pm 0.60) \times 2$
Frequency shift in the doubling crystal	$< \pm 0.35$
ac Stark shift by the 397 nm laser	$(-1.27 \pm 0.64) \times 2$
dc Stark shift by the stray electric field	$(+0.77 \pm 0.39) \times 2$
Pressure shift	$< +0.10 \pm 0.05$
Sum and uncertainty in quadrature	-10.4 ± 2.0

[a]Reference 5.

in Fig. 4, which also illustrates how the center frequency of the transition was obtained.

The frequency difference between the two scans of each pair amounted to $\sim 2 \times 50$ MHz, and the mean wave number of the transition to the $54p1_1(0)$ level was determined to be $2 \times 12\,604.998\,80(10)$ cm^{-1}, where the number in parentheses represents one standard deviation in the unit of the last digit.

Additional corrections to the calibrated frequency listed above and the associated uncertainties had to be considered. (i) A possible frequency shift arising in the doubling crystal as a result of the Kerr effect[20] and/or a phase-mismatch in the crystal.[17,21] The shift resulting from these two effects under our experimental conditions (pulse length of ~ 70 ns, crystal length of 5 mm, and peak intensity in the NIR of 2.4×10^7 W/cm^2) is -1 kHz for the Kerr effect and less than ± 350 kHz for the frequency shift caused by phase-mismatch, assuming the phase-mismatch $\Delta k < 0.3$ mm^{-1}, which corresponds to a 20% decrease in the conversion efficiency from its maximum value. (ii) The ac Stark shift induced by the 397 nm laser was determined by varying the laser pulse energies and extrapolating the transition frequencies. Because the 202 nm laser pulses preceded the 397 nm laser pulses, no ac Stark shift needed to be considered for this laser. (iii) The dc Stark shift resulting from residual stray electric fields was measured by applying different offset voltages to the metallic plates surrounding the photoionization region. The magnitude of the stray field and the dc Stark shift were deduced from the second-order polynomial fit of the frequency shift as a function of the offset voltages.[22,23] (iv) The pressure shift was estimated to be less than 0.1 MHz from the pressure-shift coefficient of Rydberg states of H_2 reported by Herzberg and Jungen[24] [5.7 ± 0.5 cm^{-1}/amagat (1 amagat$=2.686\,777\,4(47) \times 10^{19}$ cm^{-3})] and the local concentration ($\sim 10^{13}$ cm^{-3}) of the hydrogen molecules in the interaction region under the present experimental conditions. The uncertainties of the ac and dc Stark shifts and pressure shift were assumed to be half the absolute value, which represents a conservative estimate. Other sources of errors and uncertainties related to the frequency calibration were also taken into account as indicated in Table I. The wave number of the $54p1_1(0) \leftarrow EF\ ^1\Sigma_g^+(v=0,N=1)$ transition was determined to be $25\,209.997\,56 \pm (0.000\,22)_{\text{statistical}} \pm (0.000\,07)_{\text{systematic}}$ cm^{-1}, which represents the main experimental result of this article. This result includes the -10.4 MHz correction resulting from the systematic shifts listed in Table. I. By adding the statistical and systematic errors, the result can be given as $25\,209.997\,56(29)$ cm^{-1}. The experimental precision is limited mainly by the statistical uncertainty in the determination of the centers of the H_2 lines and the systematic uncertainty in the frequency shift arising in the Ti:Sa amplifier.

B. The ionization energy of H_2

Figure 1 illustrates the energy level diagram used in the determination of the ionization energies of ortho- and para-H_2. The numerical values of all relevant wave number intervals are listed in Table II and lead to a value of $124\,357.237\,97(36)$ cm^{-1} for the ionization energy of ortho-H_2. This value corresponds to the center of gravity of the hyperfine structure components of the $N^+=1$ level of H_2^+.[25] The $54p1_1(0)$ level has three hyperfine components, separated by $\sim 0.000\,11$ and $\sim 0.000\,05$ cm^{-1} as determined from the transition frequencies in Ref. 6, and were not resolved in the present experiment. Their mean value has been used in the present calculation, resulting in an uncertainty of less than 0.0001 cm^{-1}. The three hyperfine levels of the $X\ ^1\Sigma_g^+(v=0,N=1)$ level are split by less than 500 kHz;[26] the hyperfine splittings of the $EF\ ^1\Sigma_g^+(v=0,N=1)$ level are assumed to be equally small and thus negligible for the present analysis. The overall uncertainty in the ionization energy of ortho-H_2 is determined as quadrature summation of the uncertainties of all energy level intervals. Using the energy separations between the $N=0$ and $N=1$ levels of the $X\ ^1\Sigma_g^+(v=0)$ state of H_2 (Ref. 8) and that between the

TABLE II. Energy level intervals and determination of the ionization energy of H_2 in cm^{-1}.

	Energy level interval	Wave number (cm^{-1})	Ref.
(1)	$X\ ^1\Sigma_g^+(v=0,N=1)-X\ ^1\Sigma_g^+(v=0,N=0)$	118.486 84(10)	8
(2)	$EF\ ^1\Sigma_g^+(v=0,N=1)-X\ ^1\Sigma_g^+(v=0,N=1)$	99 109.731 39(18)	5
(3)	$54p1_1(S=0,\text{center})-EF\ ^1\Sigma_g^+(v=0,N=1)$	25 209.997 56(29)	This work
(4)	$54p1_1(S=0),F=1-51d1_1(G^+=1/2),F=0$	4.791 80	6
(4)	$54p1_1(S=0),F=0-51d1_1(G^+=1/2),F=0$	4.791 91	6
(4)	$54p1_1(S=0),F=2-51d1_1(G^+=1/2),F=0$	4.791 96	6
(5)	$X^+\ ^2\Sigma_g^+(v^+=0,N^+=1,G^+=1/2),F^+=1/2-51d1_1(G^+=1/2),F=0$	42.270 539(10)	6
(6)	$X^+\ ^2\Sigma_g^+(v^+=0,N^+=1,\text{center})-X^+\ ^2\Sigma_g^+(v^+=0,N^+=1,G^+=1/2),F^+=1/2$	0.030 379 61	25
(7)	$X^+\ ^2\Sigma_g^+(v^+=0,N^+=1,\text{center})-X^+\ ^2\Sigma_g^+(v^+=0,N^+=0)$	58.233 675 1(1)	9–11

$E_i(\text{ortho-}H_2)=(2)+(3)-(4)+(5)+(6)=124\ 357.237\ 97(36)$
$E_i(H_2)\equiv E_i(\text{para-}H_2)=(1)+E_i(\text{ortho-}H_2)-(7)=124\ 417.491\ 13(37)$

$N^+=0$ and $N^+=1$ levels of the $X^+\ ^2\Sigma_g^+(v^+=0)$ state of H_2^+,[9–11] the ionization energy of para-H_2 can be determined to be 124 417.491 13(37) cm^{-1}.

The precision of the present value exceeds that of the latest theoretical results.[4] Our new result thus represents a test for future calculations of $E_i(H_2)$ and also of $D_0(H_2)$ in combination with precise values of $E_i(H)$ and $D_0(H_2^+)$ as explained in more detail in the next subsection.

C. The dissociation energy of H_2

The relationship between the dissociation energy $D_0(H_2)$ and the ionization energy $E_i(H_2)$ of molecular hydrogen [Eq. (1)] is depicted graphically in Fig. 5. As part of our procedure to obtain an improved value of $D_0(H_2)$ from our new value of $E_i(H_2)$, we have reevaluated the ionization energy of atomic hydrogen $E_i(H)$ and the dissociation energy of the hydrogen molecular cation $D_0(H_2^+)$ using the most recent values of the fundamental constants recommended in CODATA 2006,[27] i.e., $R_\infty=109\ 737.315\ 685\ 27(73)$ cm^{-1} for the Rydberg constant and $\mu=M_p/m_e=1836.152\ 672\ 47(80)$ for the proton-to-electron mass ratio, and the global average of the fine structure constant $\alpha=1/137.035\ 999\ 679\ 082(45)$ including the results of the most recent measurements.[27,28] The uncertainties in the values of $E_i(H)$ and $D_0(H_2^+)$ make a negligible contribution to the final uncertainty of $D_0(H_2)$, which is dominated by the experimental uncertainty of $E_i(H_2)$.

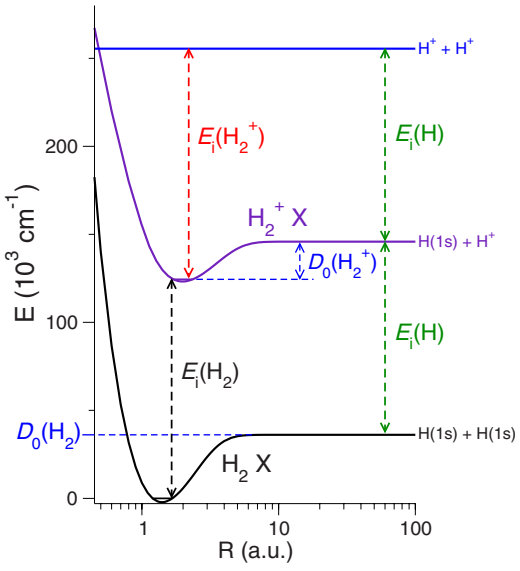

FIG. 5. (Color online) Potential energy diagram showing the potential energy functions of the $X\ ^1\Sigma_g^+$ ground state of H_2 and the $X^+\ ^2\Sigma_g^+$ ground state of H_2^+ and illustrating the relationship between the various ionization and dissociation energies.

The atomic ionization energy $E_i(H)$ is defined as the energy interval between the ionization limit and the atomic ground state ($1\ ^2S_{1/2}$) without the effects of the hyperfine interactions.[7] The center of gravity of the hyperfine structure of the $1\ ^2S_{1/2}$ ground state of H lies 1 065 304.313 826 0(75) kHz $(=(3/4)\Delta_{hfs})$ above the lowest $(F=0)$ hyperfine level. To obtain this value, we have used the hyperfine splitting Δ_{hfs} reported in Ref. 29. The present method of determining $E_i(H)$ represents the inverse of the method used in the determination of the Rydberg constant from spectroscopic measurements on atomic hydrogen as discussed by Biraben.[30] The atomic level energy is expressed as a sum of three terms,

$$E_{n,l,j}=E_{n,j}^{\text{Dirac}}+E_n^{\text{recoil}}+L_{n,l,j}. \tag{2}$$

The first term, $E_{n,j}^{\text{Dirac}}$, is the Dirac energy eigenvalue for a particle with a reduced mass $m_r=m_e(1+m_e/M_p)^{-1}$. The second term, E_n^{recoil}, is the first relativistic recoil correction associated with the finite mass of the proton. $L_{n,l,j}$ is the Lamb shift term accounting for all other corrections, including QED corrections, higher-order relativistic corrections, and the effects resulting from the proton structure.

The atomic level energy (relative to the ionization limit) obtained from the nonrelativistic Schrödinger equation is

$$E_n^{\text{NR}}=-\frac{Z^2}{n^2}hcR_\infty, \tag{3}$$

where Z is the charge number of the nucleus ($Z=1$ in the present case) and n is the principal quantum number. To account for the finite mass of the proton, the electron mass m_e is replaced by the reduced mass m_r, resulting in the relativistic Dirac eigenvalue with the reduced mass correction[7,27]

$$E_{n,j}^{\mathrm{Dirac}} = \left(\frac{m_r}{m_e}\right) E_n^{\mathrm{NR}} \left(1 - \left[1 + \left(\frac{Z\alpha}{n-\delta}\right)^2\right]^{-1/2}\right) \frac{2n^2}{(Z\alpha)^2}, \quad (4)$$

where $\delta = (j+1/2) - \sqrt{(j+1/2)^2 - (Z\alpha)^2}$. The first relativistic correction associated with the proton recoil can be expressed as[7,30]

$$E_n^{\mathrm{recoil}} = E_n^{\mathrm{NR}} \frac{m_r^2}{m_e(m_e+M_p)} \left(\frac{Z\alpha}{2n}\right)^2. \quad (5)$$

Higher-order relativistic recoil corrections (e.g., of the QED terms) are included in the Lamb shift term.

We have recalculated the Lamb shift corrections using the formulae detailed in CODATA 2006 (Ref. 27) and the values of fundamental constants mentioned above and find the following contributions to the binding energy ($-E_i(\mathrm{H})$) of the "hyperfineless" $1\ ^2S_{1/2}$ ground state

$$E_{1S_{1/2}}^{\mathrm{Dirac}} = -109\,679.043\,564\,75(73)\ \mathrm{cm}^{-1}, \quad (6)$$

$$E_{1S_{1/2}}^{\mathrm{recoil}} = -0.000\,794\,340\,7\ \mathrm{cm}^{-1}, \quad (7)$$

$$L_{1S_{1/2}} = 0.272\,616\,53(67)\ \mathrm{cm}^{-1}, \quad (8)$$

where the uncertainty in the recoil term is on the order of 4×10^{-13} cm^{-1} and thus entirely negligible. The uncertainty in the Lamb shift term is dominated by the uncertainty contributions of R_∞ and the proton radius. The updated atomic hydrogen ionization energy is thus

$$E_i(\mathrm{H}) = 109\,678.771\,742\,6(10)\ \mathrm{cm}^{-1}. \quad (9)$$

The present value for $E_i(\mathrm{H})$ is comparable with that of Wolniewicz[4] (109 678.7717 cm^{-1}), where no uncertainty was indicated. Wolniewicz[4] used a recent value for R_∞, with an unspecified value, in order to correct (or rescale) the value tabulated by Erickson[7] (109 678.773 704(3) cm^{-1}), the uncertainty of which only includes the uncertainty in the Lamb shift term but does not include the uncertainty of 8.3×10^{-3} cm^{-1} in R_∞.

The one-electron molecular ion H_2^+ is the simplest test system of *ab initio* molecular quantum theory. In the nonrelativistic approximation, the level energies have been calculated to precisions of up to $10^{-30}\ E_h$.[31] Despite its apparent simplicity, the three-body system represents a formidable problem, which poses particular difficulties in accounting for relativistic and radiative corrections to the level energies. The dissociation energy $D_0(H_2^+)$ is defined relative to the hyperfineless ground state $(v^+=0, N^+=0)$ of H_2^+. We used the formulae reported by Korobov[9–11] to determine the H_2^+ ground state $(v^+=0, N^+=0)$ energy relative to the onset of the dissociation continuum, which should result in a slight improvement over the calculations of Moss.[32] In *ab initio* calculations, the level energies are determined relative to $E_i(H_2^+)$, the ionization energy of the molecular ion H_2^+. Included in the present reevaluation are the energy corrections comprising relativistic and radiative terms of up to $\mathcal{O}(\alpha^5 R_\infty)$ from Refs. 9–11. We used the same values for the fundamental constants as in the reevaluation of $E_i(\mathrm{H})$ described above and obtained

$$E_i(H_2^+) = 131\,058.121\,975(49)\ \mathrm{cm}^{-1}. \quad (10)$$

The indicated uncertainty is not limited by the uncertainties of the fundamental constants used but by the fact that higher-order terms were neglected. The uncertainties obtained for molecular rovibrational transition energies are much smaller (see, e.g., Ref. 11) because the contributions from the neglected terms are expected to be almost equal for different rovibrational states and therefore largely cancel.

Using the relation $E_i(H_2^+) = D_0(H_2^+) + E_i(\mathrm{H})$ (see Fig. 5), we obtain a value for the dissociation energy of the molecular ion,

$$D_0(H_2^+) = 21\,379.350\,232(49)\ \mathrm{cm}^{-1}, \quad (11)$$

where the uncertainty of $E_i(\mathrm{H})$ makes a negligible contribution to the final uncertainty. The present value of $D_0(H_2^+)$ agrees well with that previously derived by Moss[32] (21 379.3501(1) cm^{-1}).

Using the calculated values for $E_i(\mathrm{H})$, $E_i(H_2^+)$, $D_0(H_2^+)$, and the experimental value of $E_i(H_2)$, the dissociation energy of H_2 can be derived from Eq. (12) or Eq. (13),

$$D_0(H_2) = E_i(H_2) + D_0(H_2^+) - E_i(\mathrm{H}), \quad (12)$$

$$= E_i(H_2) + E_i(H_2^+) - 2E_i(\mathrm{H}), \quad (13)$$

$$= 36\,118.069\,62(37)\ \mathrm{cm}^{-1}. \quad (14)$$

The final uncertainty in $D_0(H_2)$ is entirely limited by the experimental uncertainty of $E_i(H_2)$, and indeed we would have obtained the same value had we used the values of $D_0(H_2^+)$ and $E_i(\mathrm{H})$ reported in Refs. 4, 7, and 32 rather than the updated values given in Eqs. (11) and (9).

The present value of the dissociation energy $D_0(H_2)$ is consistent with, but more precise than, the result of the *ab initio* calculations of Wolniewicz[4] $(D_0(H_2)_{\mathrm{th}} = 36\,118.069$ cm$^{-1})$ and the most recent experimental result of Zhang *et al.*[3] $(D_0(H_2)_{\mathrm{exp}} = 36\,118.062(10)$ cm$^{-1})$.

IV. CONCLUSIONS

Table III and Fig. 6 summarize the results of determinations, by various methods, of the ionization energy of para-H_2 over the past 40 years. Because of the relationship between the dissociation and ionization energies of H_2 [Eq. (1)], the recommended value of the dissociation energy has evolved in a very similar manner. Earlier determinations of the dissociation energy have been summarized in Ref. 1. Compared to previous experimental values of the dissociation and ionization energies of H_2, the present values (36 118.069 62(37) cm^{-1} and 124 417.491 13(37) cm^{-1}, respectively) are more precise by a factor of ~30.

As part of the procedure of determining the dissociation energy, we have attempted to reevaluate the ionization energy of H and the dissociation energy of H_2^+ using the latest values of the fundamental constants α, M_p/m_e, and R_∞. The main result of this reevaluation is that the current uncertainties in these quantities make a negligible contribution to the uncertainty of the dissociation energy of H_2, which is entirely determined by the uncertainty of the ionization energy of H_2.

TABLE III. $E_i(H_2)$ as determined in various experimental and theoretical studies or combinations thereof, in cm^{-1}.

Year	Expt. (cm^{-1})	Theor. (cm^{-1})	Ref.
1969	124 418.4(4)		33
1969		124 418.3	33
1972	124 417.2(4)		24
1986	124 417.51(22)		34
1987	124 417.61(7)		35
1987	124 417.42(15)		34, revised in 36
1987	124 417.53(7)		35, revised in 36
1989	124 417.524(15)		37
1990	124 417.501(17)		38
1992	124 417.507(18)		39
1993		124 417.471	40
1993	124 417.507(12)		37, revised in 41
1993	124 417.484(17)		38, revised in 41
1993		124 417.482	42
1994	124 417.488(10)		43
1994		124 417.496	44
1995		124 417.491	4
2002	124 417.476(12)		2
2008	124 417.491 13(37)		This work

Our new values of the ionization and dissociation energies of molecular hydrogen are in excellent agreement with the latest theoretical results, 124 417.491 cm^{-1} for the ionization energy and 36 118.069 cm^{-1} for the dissociation energy,[4] which included adiabatic, nonadiabatic, relativistic, and radiative corrections to the Born–Oppenheimer energies, and are believed to be accurate to within 0.01 cm^{-1}. The new value of the ionization energy can be regarded as the most precise and accurate experimental result of this quantity, whereas the dissociation energy is a hybrid experimental-theoretical determination. Because of their higher precision, the present results represent an incentive to improve calculations of the ionization and dissociation energies beyond the current limits.

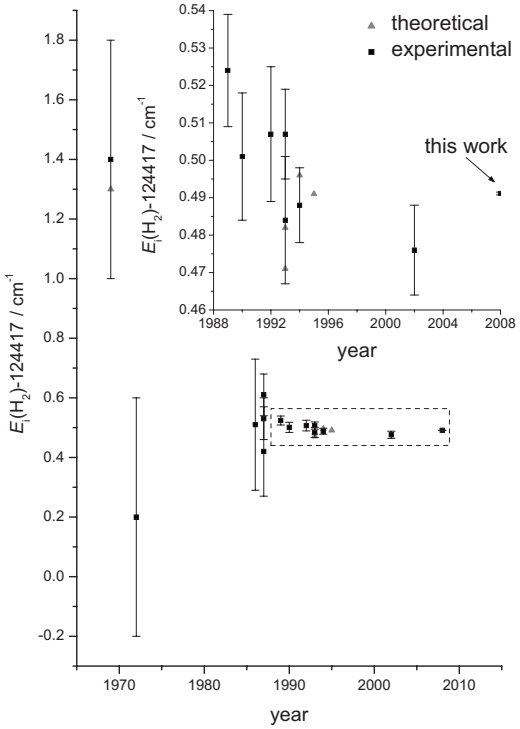

FIG. 6. Values for the ionization energy of H_2 as determined in various studies or combinations thereof. The inset is an enlargement of the dashed frame and provides a better view of the evolution over the past 20 years.

ACKNOWLEDGMENTS

The authors thank Dr. H. Knöckel (Hannover) for providing them with the iodine cell and for important discussions on frequency calibration issues. This work was financially supported by the European Research Council (ERC Grant No. 228286), the Swiss National Science Foundation under Project No. 200020-116245, the Netherlands Foundation for Fundamental Research of Matter (FOM), and Laserlab-Europe (Grant No. RII3-CT-2003-506350). J.K. acknowledges financial support from the Netherlands Organisation for Scientific Research (NWO).

[1] H. Primas and U. Müller-Herold, *Elementare Quantenchemie* (Teubner Studienbücher, Stuttgart, 1984) gives a complete account of the early efforts invested in the quantitative comparison of experimental and theoretical values of the dissociation energy of H_2 and explains in detail how studies of molecular hydrogen contributed to establish the validity of molecular quantum mechanics and to understand chemical bonds physically.
[2] A. de Lange, E. Reinhold, and W. Ubachs, Phys. Rev. A **65**, 064501 (2002).
[3] Y. P. Zhang, C. H. Cheng, J. T. Kim, J. Stanojevic, and E. E. Eyler, Phys. Rev. Lett. **92**, 203003 (2004).
[4] L. Wolniewicz, J. Chem. Phys. **103**, 1792 (1995).
[5] S. Hannemann, E. J. Salumbides, S. Witte, R. T. Zinkstok, E.-J. van Duijn, K. S. E. Eikema, and W. Ubachs, Phys. Rev. A **74**, 062514 (2006).
[6] A. Osterwalder, A. Wüest, F. Merkt, and Ch. Jungen, J. Chem. Phys. **121**, 11810 (2004).
[7] G. W. Erickson, J. Phys. Chem. Ref. Data **6**, 831 (1977).
[8] D. E. Jennings, S. L. Bragg, and J. W. Brault, Astrophys. J. **282**, L85 (1984).
[9] V. I. Korobov, Phys. Rev. A **73**, 024502 (2006).
[10] V. I. Korobov, Phys. Rev. A **74**, 052506 (2006).
[11] V. I. Korobov, Phys. Rev. A **77**, 022509 (2008).
[12] R. Seiler, Th. Paul, M. Andrist, and F. Merkt, Rev. Sci. Instrum. **76**, 103103 (2005).
[13] Th. A. Paul and F. Merkt, J. Phys. B **38**, 4145 (2005).
[14] Th. A. Paul, H. A. Cruse, H. J. Wörner, and F. Merkt, Mol. Phys. **105**, 871 (2007).
[15] H. Knöckel, B. Bodermann, and E. Tiemann, Eur. Phys. J. D **28**, 199 (2004).
[16] I. Reinhard, M. Gabrysch, B. F. von Weikersthal, K. Jungmann, and G. zu Putlitz, Appl. Phys. B: Lasers Opt. **63**, 467 (1996).
[17] N. Melikechi, S. Gangopadhyay, and E. E. Eyler, J. Opt. Soc. Am. B **11**, 2402 (1994).
[18] K. F. Wall, R. L. Aggarwal, M. D. Sciacca, H. J. Zeiger, R. E. Fahey, and A. J. Strauss, Opt. Lett. **14**, 180 (1989).
[19] T. A. Planchon, W. Amir, C. Childress, J. A. Squier, and C. G. Durfee, Opt. Express **16**, 18557 (2008).
[20] H. Li, F. Zhou, X. Zhang, and W. Ji, Opt. Commun. **144**, 75 (1997).
[21] A. V. Smith and M. S. Bowers, J. Opt. Soc. Am. B **12**, 49 (1995).
[22] M. Schäfer and F. Merkt, Phys. Rev. A **74**, 062506 (2006).
[23] A. Osterwalder and F. Merkt, Phys. Rev. Lett. **82**, 1831 (1999).
[24] G. Herzberg and Ch. Jungen, J. Mol. Spectrosc. **41**, 425 (1972).
[25] J.-P. Karr, F. Bielsa, A. Douillet, J. P. Gutierrez, V. I. Korobov, and L. Hilico, Phys. Rev. A **77**, 063410 (2008).
[26] N. F. Ramsey, Phys. Rev. **85**, 60 (1952).
[27] P. J. Mohr, B. N. Taylor, and D. B. Newell, Rev. Mod. Phys. **80**, 633 (2008).
[28] D. Hanneke, S. Fogwell, and G. Gabrielse, Phys. Rev. Lett. **100**, 120801 (2008); G. Gabrielse, D. Hanneke, T. Kinoshita, M. Nio, and B. Odom, *ibid.* **99**, 039902 (2007); G. Gabrielse, D. Hanneke, T. Kinoshita, M. Nio,

and B. Odom, *ibid.* **97**, 030802 (2006); M. Cadoret, E. de Mirandes, P. Clade, S. Guellati-Khelifa, C. Schwob, F. Nez, L. Julien, and F. Biraben, *ibid.* **101**, 230801 (2008); P. Clade, E. de Mirandes, M. Cadoret, S. Guellati-Khelifa, C. Schwob, F. Nez, L. Julien, and F. Biraben, Phys. Rev. A **74**, 052109 (2006); V. Gerginov, K. Calkins, C. E. Tanner, J. J. McFerran, S. Diddams, A. Bartels, and L. Hollberg, *ibid.* **73**, 032504 (2006).
[29] S. G. Karshenboim, Phys. Rep. **422**, 1 (2005).
[30] F. Biraben, e-print arXiv:0809.2985v1.
[31] H. Li, J. Wu, B.-L. Zhou, J.-M. Zhu, and Z.-C. Yan, Phys. Rev. A **75**, 012504 (2007).
[32] R. E. Moss, Mol. Phys. **80**, 1541 (1993).
[33] G. Herzberg, Phys. Rev. Lett. **23**, 1081 (1969).
[34] E. E. Eyler, R. C. Short, and F. M. Pipkin, Phys. Rev. Lett. **56**, 2602 (1986).
[35] W. L. Glab and J. P. Hessler, Phys. Rev. A **35**, 2102 (1987).
[36] E. E. Eyler, J. Gilligan, E. McCormack, A. Nussenzweig, and E. Pollack, Phys. Rev. A **36**, 3486 (1987).
[37] E. McCormack, J. M. Gilligan, C. Cornaggia, and E. E. Eyler, Phys. Rev. A **39**, 2260 (1989).
[38] Ch. Jungen, I. Dabrowski, G. Herzberg, and M. Vervloet, J. Chem. Phys. **93**, 2289 (1990).
[39] J. M. Gilligan and E. E. Eyler, Phys. Rev. A **46**, 3676 (1992).
[40] W. Kołos and J. Rychlewski, J. Chem. Phys. **98**, 3960 (1993).
[41] D. Shiner, J. M. Gilligan, B. M. Cook, and W. Lichten, Phys. Rev. A **47**, 4042 (1993).
[42] L. Wolniewicz, J. Chem. Phys. **99**, 1851 (1993).
[43] J.-C. D. Meiners, M.S. thesis, University of Delaware, 1994.
[44] W. Kołos, J. Chem. Phys. **101**, 1330 (1994).